High-precision and high-accuracy rovibrational spectroscopy of molecular ions

James N. Hodges, Adam J. Perry, Paul A. Jenkins, Brian M. Siller, and Benjamin J. McCall

Additional information on J. Chem. Phys.
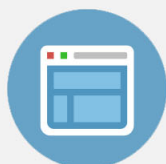
High-precision and high-accuracy rovibrational spectroscopy of molecular ions

James N. Hodges,[1] Adam J. Perry,[1] Paul A. Jenkins II,[1] Brian M. Siller,[1,a)] and Benjamin J. McCall[1,2,b)]

[1]*Department of Chemistry, University of Illinois, Urbana, Illinois 61801, USA*
[2]*Departments of Astronomy and Physics, University of Illinois, Urbana, Illinois 61801, USA*

We present a versatile new instrument capable of measuring rovibrational transition frequencies of molecular ions with sub-MHz accuracy and precision. A liquid-nitrogen cooled positive column discharge cell, which can produce large column densities of a wide variety of molecular ions, is probed with sub-Doppler spectroscopy enabled by a high-power optical parametric oscillator locked to a moderate finesse external cavity. Frequency modulation (heterodyne) spectroscopy is employed to reduce intensity fluctuations due to the cavity lock, and velocity modulation spectroscopy permits ion-neutral discrimination. The relatively narrow Lamb dips are precisely and accurately calibrated using an optical frequency comb. This method is completely general as it relies on the direct measurement of absorption or dispersion of rovibrational transitions. We expect that this new approach will open up many new possibilities: from providing new benchmarks for state-of-the-art *ab initio* calculations to supporting astronomical observations to helping assign congested spectra by combination differences. Herein, we describe the instrument in detail and demonstrate its performance by measuring ten R-branch transitions in the ν_2 band of H_3^+, two transitions in the ν_1 band of HCO^+, and the first sub-Doppler transition of CH_5^+. © *2013 AIP Publishing LLC*. [http://dx.doi.org/10.1063/1.4825251]

I. INTRODUCTION

In the 30 years since its discovery,[1] velocity modulation spectroscopy (VMS) in a positive column discharge has been a tremendously successful method for performing direct absorption spectroscopy of molecular ions. The positive column offers a remarkably rich chemical environment suitable for the production of a wide variety of ions with a high column density.[2]

Traditional VMS has been limited in its frequency precision by broad Doppler-limited linewidths, coupled with modest signal-to-noise ratios, and the uncertainties in line center determinations are typically 30-90 MHz.[3,4] The Doppler limit was overcome by our group in 2010 by placing the discharge cell in an external cavity, in an approach called cavity enhanced VMS.[5,6] The high intracavity power enabled saturation spectroscopy, and the resulting Lamb dips enabled the precision to be improved to ~3 MHz in the near-infrared. The later incorporation of frequency modulation, or heterodyne, spectroscopy improved the signal-to-noise ratio and further improved the precision.[7] This approach, based on the pioneering NICE-OHMS technique,[8] was dubbed NICE-OHVMS, or Noise Immune Cavity Enhanced Optical Heterodyne Velocity Modulation Spectroscopy. This technique was later extended into the mid-infrared, using an optical parametric oscillator, by Crabtree *et al.*[9]

The accuracy of VMS has also been limited by the method of frequency calibration. Typically, VMS experiments relied on a combination of relative calibration using marker etalons and absolute calibration using Doppler-limited reference gas transitions, which were themselves often only known to ~30 MHz accuracy. The advent of optical frequency combs has revolutionized the accuracy of molecular spectroscopy, making sub-MHz frequency measurements almost routine. Our near-infrared NICE-OHVMS work on N_2^+ used a frequency comb to achieve an accuracy of ~300 kHz.[7] In recent work without an external cavity, we have demonstrated that it is possible to extend comb-calibrated spectroscopy to the mid-infrared, to infer pure-rotational transitions of molecular ions such as HCO^+ using combination differences with sub-MHz accuracy.[10]

In this paper, we present the combination of sub-Doppler spectroscopy using mid-infrared NICE-OHVMS[9] with optical frequency comb calibration[10] to yield a versatile method for molecular ion spectroscopy with both high precision and high accuracy. We demonstrate and characterize the effectiveness of this method through spectroscopy of H_3^+, HCO^+, and CH_5^+.

H_3^+ is a natural first target for our spectrometer. As the simplest polyatomic molecule, it has become an important system for benchmarking the increasing accuracy of quantum calculations. Many of its rovibrational transitions have been predicted to within hundredths of a wavenumber by sophisticated calculations that include adiabatic, relativistic electron, and non-adiabatic corrections to the Born-Oppenheimer potential energy surface.[11] In many cases, this degree of precision is comparable to the experimental uncertainties, so more precise measurements will serve to motivate and benchmark ever more accurate calculations, which will require the
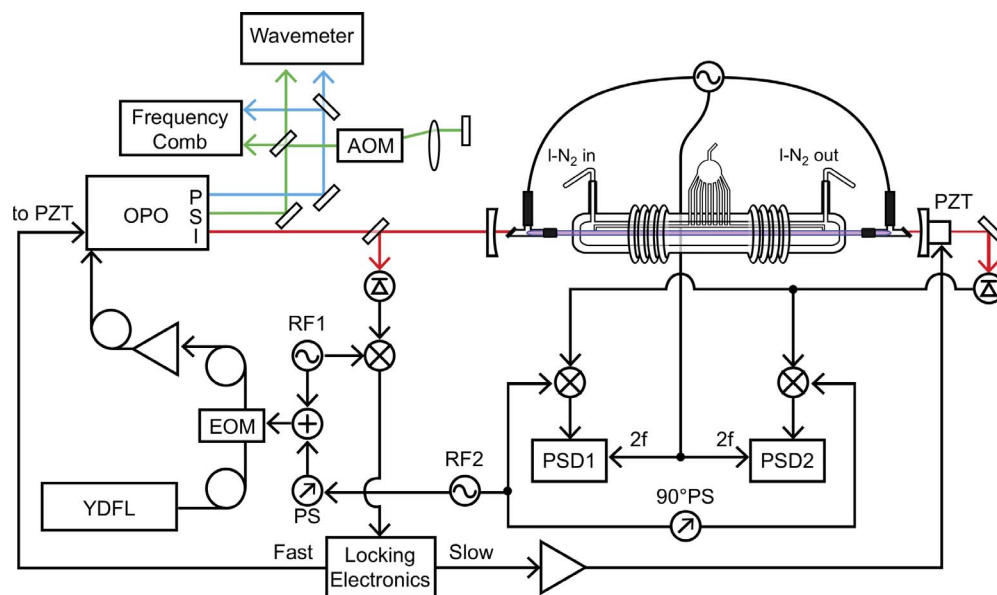
FIG. 1. Block diagram of the instrument. YDFL: Ytterbium Doped Fiber Laser; EOM: Electro-Optic Modulator; OPO: Optical Parametric Oscillator; P,S,I: Pump(Blue), Signal(Green), Idler(Red); AOM: Acousto-Optic Modulator; PZT: Piezo-electric Transducer; PS: Phase Shifter; RF: Radio-Frequency source; and PSD: Phase Sensitive Detector.

inclusion of quantum electrodynamic effects as has already been done with diatomics[12] and H_2O.[13]

In addition to its fundamental interest, H_3^+ is also an important molecule in astrochemistry due to its abundance in both dense[14] and diffuse[15] interstellar clouds, as well as in the atmospheres of large gas giants such as Jupiter.[16] Of particular relevance to the present work, the Doppler shifts of H_3^+ rovibrational transitions have been successfully used to determine the velocity of Jovian auroral winds,[17] but the accuracy of those determinations is limited by the uncertainties in the laboratory transition frequencies.

Our second target, HCO^+, was recently used[10] to demonstrate the feasibility of performing "indirect" pure-rotational spectroscopy by calculating combination differences of high-precision rovibrational frequencies. Due to degradation of our cavity mirrors in that work, we were restricted to performing single-pass heterodyne spectroscopy. Here, we revisit HCO^+ with an improved set of cavity mirrors, and we find that the single-pass measurements suffered a slight (~4 MHz) but systematic offset due to an asymmetry in the AC plasma. This highlights the advantage of using Lamb dips in a bidirectional cavity for line center determination, as they are located symmetrically around the zero-velocity component of the ions and are not shifted by plasma asymmetries.

Our final target, CH_5^+, is an enigmatic ion whose high-resolution infrared spectrum in the C–H stretching region remains completely unassigned nearly 15 years since it was first reported.[3] It has been suggested[18] that one possible way of assigning the spectrum would be to search for four-line combination differences, which would identify energy level separations. However, the high line density results in many "false positives" at the current precision of the line center measurements. Here we report the first sub-Doppler spectrum of CH_5^+, which improves on the precision of the initial detection[3] by more than two orders of magnitude.

II. EXPERIMENTAL DESCRIPTION

A block diagram of the instrument is presented in Figure 1. A ytterbium doped fiber laser (Koheras Adjustik Y-10) is coupled into a fiber electro-optic modulator (EOSPACE PM-0K5-00-PFU-PFU-106-S), where Pound Drever Hall (PDH) locking side bands (~4 MHz) and heterodyne sidebands (~79 MHz, equal to the free spectral range of our external cavity) are imprinted onto the laser. After modulation, the light is amplified by a 10 W fiber amplifier (IPG Photonics YAR-10 K-1064-LP-SF) and is used to pump a singly resonant optical parametric oscillator (OPO; Aculight Argos 2400 SF). The idler, tunable from 3.2 to 3.9 μm, is coupled into a ~190 cm external cavity composed of two dielectric mirrors (Rocky Mountain Instruments, custom) on silicon substrates with 1 m radius of curvature. For the H_3^+ measurements, the mirrors used were nominally 99.7% reflective between 3.0 and 3.4 μm but suffered high losses at higher frequencies because of water adsorbed in the hygroscopic coating. The measurements of HCO^+ and CH_5^+ have utilized a new set of mirrors, nominally 99% reflective between 3.0 and 3.4 μm, which were specially coated with a protective layer to prevent the uptake of water. Additionally, the newer mirrors are kept under a flow of dry nitrogen at all times.

The cavity and the idler are locked to maintain resonance by using a detector (Boston Electronics Vigo PVM-10.6-1x1) to monitor the back reflection from the front cavity mirror. The signal from that detector is demodulated with a mixer that is referenced to the PDH locking sideband frequency. The output of that mixer is processed by a lock box, and slow corrections (<100 Hz) are sent to a piezo on which one of the cavity mirrors is mounted, to keep the cavity locked onto the idler on slow timescales. Faster corrections (0.1–10 kHz) are sent to a piezo that controls the length of the OPO cavity, thus making small corrections to the frequency of the signal and the idler

to keep the idler resonant with the cavity on fast timescales. Based on the observed magnitude of this error signal, there is an extra ~500 kHz of random noise imposed upon the signal frequency (and therefore also upon the idler frequency) due to the locking of the idler frequency to the external cavity.

Within the external cavity is a liquid nitrogen cooled positive column discharge cell (Black Widow), which was used extensively for VMS in the Oka group at the University of Chicago. An arbitrary waveform generator (Agilent 33120A) creates a sine wave, which is amplified (Techron 7780) and sent to a step-up transformer to drive the plasma. The AC voltage configuration of the plasma modulates the velocity of the ions at a frequency of 40 kHz. Optimal signals for H_3^+ have been observed at 200 mTorr of cell pressure and 170 mA of current. For HCO^+, we used a mixture of 17:3 H_2:CO at a total pressure of 200 mTorr, and a plasma current of 115 mA. CH_5^+ was observed using a 24:1 mixture of H_2:CH_4 at 250 mTorr and the lowest possible current the discharge could maintain, typically ~110 mA.

The idler radiation from the OPO is coupled through the discharge cell by CaF_2 windows that are aligned at Brewster's angle. The transmitted light through the cavity is detected and demodulated first at the heterodyne frequency of ~79 MHz by a pair of mixers that are 90° out of phase with each other. The outputs from these mixers are further demodulated via lock-in amplifiers referenced to 80 kHz, twice the plasma modulation frequency. The detection scheme results in four data channels: in-phase and quadrature detection for each of the two mixers. Previously, we have estimated the sensitivity of our spectrometer in the lowest noise channel to be 9.8×10^{-10} cm^{-1} Hz$^{-1/2}$.[9]

Frequency calibration of the idler is accomplished by simultaneously measuring the frequency of the pump and signal beams using an optical frequency comb (Menlo Systems FC-1500, with 100 MHz repetition rate) and determining the difference between them. First, the carrier envelope offset of the comb is tuned to ~20 MHz to be measured by a frequency counter, although this is not strictly necessary for measuring the idler frequency. The repetition rate of the comb is tuned such that the beat frequency of the signal with the comb is between 25 and 35 MHz, the range of the internal bandpass of the frequency counter used for the signal. Next, the pump is tuned so that its beat with the comb is ~20 MHz. Then the signs of the beats and carrier envelope offset are determined. The pump is then offset locked to the comb using a frequency to voltage converter to generate an error signal. A wavemeter (Burleigh WA-1500, 0.2 ppm accuracy) then sequentially measures the pump and signal wavelengths to determine the mode numbers of the comb teeth that are closest to these two frequencies.

For spectroscopy, the idler is tuned by changing the repetition rate of the comb. The pump is dragged along with the comb, since it is offset-locked to the comb, but the signal remains relatively constant (aside from slow drift due to thermal variations of the OPO cavity). Without any correction, this would quickly lead to the signal beat with the comb moving out of the bandpass of our frequency counter. Therefore, we double-pass the signal through an acousto-optic modulator (Brimrose IPF-200-80-1600) before sending it to the beat

detection unit of the comb. The AOM frequency is adjusted with a feed forward as the comb repetition rate is changed, in order to keep the signal beat within the bandpass. The diffraction efficiency of the AOM allows it to be tuned between 150 and 210 MHz, leading to a shift of the signal frequency by 300 to 420 MHz. When the frequency limit of the AOM is reached, the frequency is increased or decreased by 50 MHz, which corresponds to a 100 MHz change in signal frequency, and the recorded mode number for the signal is incremented or decremented appropriately. The known frequency shift induced by the AOM is subtracted from the signal frequency determined by the comb before the latter is subtracted from the pump frequency to determine the idler frequency.

Data points are acquired with a separation in time of 1.5 s, which is ample time for the lock-in amplifiers to integrate (with a time constant of 300 ms) and the frequency counters to update (at a rate of 1 Hz). These steps are taken to minimize any line dragging by delayed detection. Scanning is performed both from low to high frequency and also from high to low frequency in order to remove any systematic errors caused by line dragging.

The use of the repetition rate for tuning limits the width of a single scan window to ~900 MHz. In practice, this means that entire Doppler profiles of light ions such as H_3^+ cannot be measured in a single scan. In such cases, preliminary scans are taken without the frequency comb (by directly scanning the voltage on the fiber laser) over a wide range, and then the sub-Doppler features are scanned with the comb. For the heavier ions HCO^+ and CH_5^+, it is possible to record the full Doppler profile within a single scan.

III. RESULTS AND DISCUSSION

A. Lineshape fitting and uncertainty determination

The symmetry of the overall NICE-OHVMS lineshape is odd in both absorption and dispersion. For high precision line center determination, the most important part of the line is the Lamb dips that are evenly spaced about the transition's center frequency. The Lamb dips are a result of the forward- and counter-propagating beam sampling single velocity components on opposite sides of the Doppler profile. The frequency modulation effectively produces three lasers spaced by the modulation frequency: a carrier and two sidebands, one in phase with the carrier, and the other 180° out of phase. Assuming that both the carrier and sidebands are intense enough to contribute to saturation, and that the modulation index is low enough to avoid contributions of higher-order sidebands, there exist four separate Lamb dips that can be detected in absorption, spaced evenly in half integer multiples of the heterodyne frequency about the linecenter. In dispersion, there is also a fifth Lamb dip at the linecenter. In this work, detection was performed at a blended phase that provided the optimal signal-to-noise in all four channels, so the observed Lamb dips are from neither purely absorption nor purely dispersion. However, these individual Lamb dips are not resolved in this experiment because half of the heterodyne frequency is smaller than the full-width at half-maximum of the individual Lamb dips; thus we observe a blend of the five Lamb dips. For
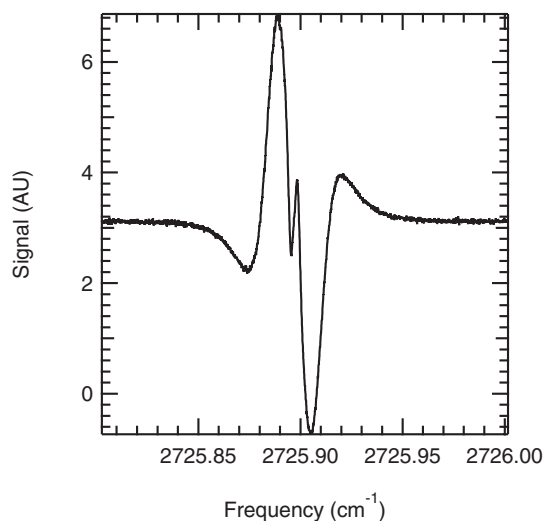
FIG. 2. A representative scan of the R(1,0) transition of H_3^+, illustrating the odd symmetry of the Doppler broadened lineshape. The sharp central feature is composed of five blended Lamb dips. This spectrum was only calibrated with a wavemeter, limiting its accuracy to 70 MHz.

purposes of illustration, the full profile from a single detection channel (not comb calibrated) of an H_3^+ transition is shown in Figure 2, and an example of the fit to the blended Lamb dips in all four simultaneously acquired detection channels is shown in Figure 3.

The derivation of the sub-Doppler lineshape and the fits function have been presented in an earlier paper.[9] However, for clarity, the fitting procedure will be reviewed in brief. The fit is a nonlinear least squares fit using an equation that models the Lamb dips and fits the central portion of the Doppler profile with a cubic polynomial. The four individual channels are fit simultaneously with some shared parameters such as the linecenter to make the four fits self-consistent. The equation describing the Lamb dip shape is a sum of absorption and dispersion components, χ_{abs} and χ_{disp}, respectively,

$$\chi_{tot}(\nu_d) = \chi_{abs}(\nu_d) \sin \theta_h + \chi_{disp}(\nu_d) \cos \theta_h, \qquad (1)$$

$$\chi_{abs}(\nu_d) = A_1 \left[\chi \left(\nu_d - \frac{f_h}{2} \right) - \chi \left(\nu_d + \frac{f_h}{2} \right) \right]$$
$$+ A_2 [\chi(\nu_d - f_h) - \chi(\nu_d + f_h)], \qquad (2)$$

$$\chi_{disp}(\nu_d) = -A_0 \chi(\nu_d) + A_1 \left[\chi \left(\nu_d - \frac{f_h}{2} \right) + \chi \left(\nu_d + \frac{f_h}{2} \right) \right]$$
$$+ A_2 [\chi(\nu_d - f_h) + \chi(\nu_d + f_h)]. \qquad (3)$$

Here A_n denotes the amplitude of the Lamb dip where n is the order, i.e., A_0 is the amplitude of the central Lamb dip, A_1 is the amplitude of the first set of Lamb dips out from the linecenter and so forth. The frequency detuning from the linecenter is given by ν_d, f_h is the heterodyne frequency, and
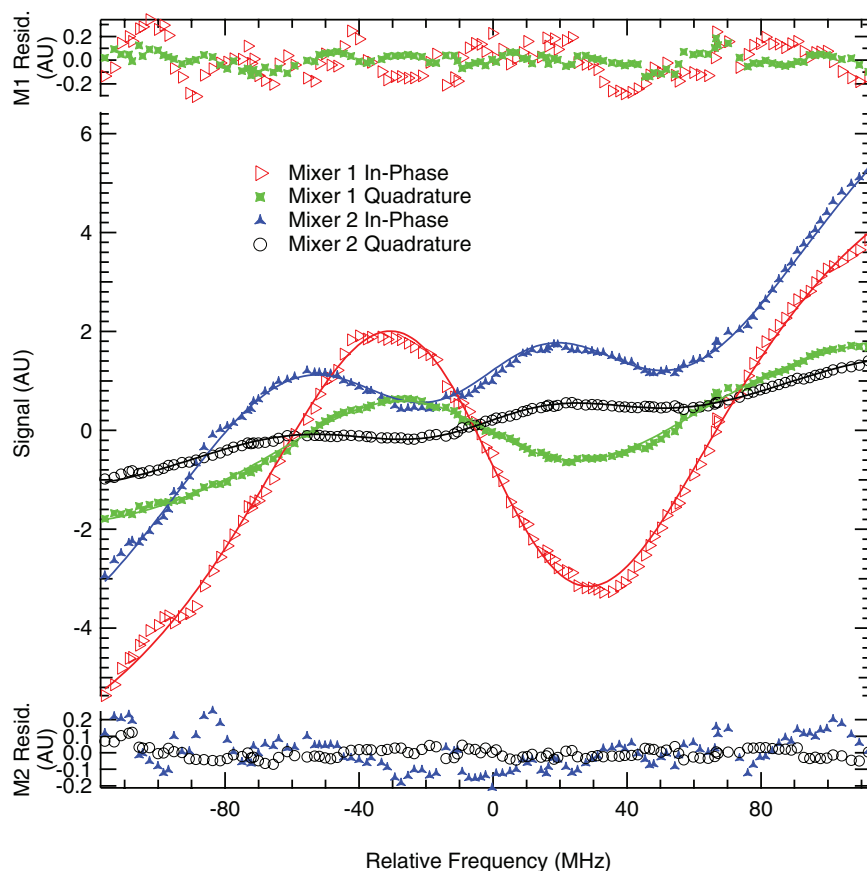

FIG. 3. Enlarged view of the Lamb dips in the R(2,2)^l transition of H_3^+, along with fits to the functional form presented in an earlier paper.[9] The four channels (two from the phase sensitive detector associated with each mixer) are presented in the center of the panel, with the residuals plotted above and below the fit. The data are shown as markers and the fits as solid lines.

θ_h is the heterodyne detection angle. The χ with no subscript is the lineshape for an individual Lamb dip, which depends on the linewidth though it is not explicitly shown in the above equations. In the case of absorption, it takes the form of a linear combination of a Lorentzian and a Gaussian. In the case of dispersion, the Lamb dips are modeled by the result of the Kramers-Krönig relation applied to the linear combination used in absorption. For more information about the fitting, we refer the reader to Crabtree *et al.*[9] Due to the blended nature of the Lamb dips, we were concerned about the potential for small changes in parameters significantly affecting the determination of the linecenter. The only part of the lineshape function that does not rely on a physical model is the fit to the central portion of the Doppler profile. Changing any of those values might make a detectable difference linecenter frequency. To simulate this, we increased the slope of the linear term in all four channels of a scan of the H_3^+ R(1,0) transition by 3 times the uncertainty in the slope returned by the original fit; this corresponds to ~3% of the total slope. The cubic term was held at zero to prevent it from compensating for the change in the linear term. This increased slope was held fixed as the data were re-fit. This simulation was repeated, decreasing the slope rather than increasing it. The linear term is the largest contributor to the polynomial part of the fit and adjusting it by 3σ in either direction only produced an error of ~27 kHz (+28 kHz for $+3\sigma$, −26 kHz for $−3\sigma$), which is well below the precision of the linecenter derived from the fit (~80 kHz) or the statistical error resulting from scan-to-scan variability (~240 kHz).

Each transition was scanned at least five times, and in some cases many more times. The linecenters determined from the fit to each scan were averaged and are reported below as the experimentally determined linecenter. The standard deviation of the individual linecenter measurements was determined and is reported to illustrate the spread of the distribution for linecenters. The standard error, also known as the standard deviation of the mean, which is simply the standard deviation divided by the square root of the number of samples, is also reported as our best estimate of the uncertainty of the average linecenter, under the assumption that the measurements are normally distributed.

B. H_3^+ spectroscopy

Our results for ten transitions of the R-branch of the ν_2 band of H_3^+ are reported in Table I. Our results are compared with those from the best available Doppler-limited spectra from the literature. In most cases, these are from the Ph.D. thesis of Wu[19] in the group of Shy, using frequency comb calibration; two transitions not observed by Wu were measured in the FTIR spectra of McKellar and Watson,[20] and the R(4,4)^l transition has not been reported since Oka's work in 1981.[21] In all cases, there is good agreement with the previous values, given the uncertainties of the latter, and in all but two cases the standard error of our measurements is sub-MHz.

With such high precision transition frequency data available, it is interesting to compare the determined transition frequencies to those previously determined to assess the quality

TABLE I. Determined line center frequencies, standard deviations, and standard errors of transitions in the ν_2 band of H_3^+. Previous values are given with the source as a footnote. The differences between the measured frequency and the previous best frequency are also reported. All values are in MHz.

Transition	Freq.	St. Dev.	St. Err.	Prev. Value	Diff.
R(1,1)^l	80687424.25	1.65	0.62	80687432(10)[a]	− 7.75
R(1,0)	81720377.29	0.86	0.23	81720370(10)[a]	7.29
R(1,1)^u	81730020.44	0.84	0.38	81730026(20)[a]	− 5.56
R(2,2)^l	82804769.99	0.70	0.31	82804764(10)[a]	5.99
R(2,1)^l	82908940.58	2.79	1.25	82908950(150)[b]	− 9.42
R(2,2)^u	84635537.25	1.21	0.54	84635542(10)[a]	− 4.75
R(2,1)^u	84724846.57	0.85	0.38	84724851(10)[a]	− 4.43
R(3,3)^l	84839013.46	0.88	0.39	84839025(10)[a]	− 11.54
R(3,2)^l	84907118.76	2.99	1.34	84907160(150)[b]	− 41.24
R(4,4)^l	86774648.52	1.28	0.39	86774570(300)[c]	78.52

[a]Reference 19.
[b]Reference 20.
[c]Reference 21.

of the older work. Especially noteworthy in this comparison is the high degree of accuracy of the FTIR work by McKellar and Watson.[20] As can be seen in Table II, their work is considerably more accurate than their stated uncertainty (150 MHz). Indeed, one of the weakest lines observed in their experiment, R(3,2)^l, is only ~40 MHz away from our determined linecenter.

There has been one other recently reported sub-Doppler measurement of the linecenter of the R(1,0) transition, from Shy's group.[22] They produce H_3^+ in an extended negative glow discharge at 30-80 mTorr and use an OPO in a strong pump, weak probe double pass configuration. Rather than scanning over the transition, calibrating each point, and fitting to determine the line center (as we have done), they instead lock their laser to the Lamb dip and use a frequency comb to measure the laser's frequency while locked. Their reported linecenter is 5.74 MHz lower than ours, a discrepancy which is far larger than the adopted uncertainties (~250 kHz in both cases). Subsequent measurements of other transitions in Shy's laboratory[23] also differ from our values, with discrepancies that vary in sign but are all of order 5 MHz.

TABLE II. A comparison to the FTIR values as determined by McKellar and Watson.[20] The error listed is the difference between our reported value and that determined by McKellar and Watson.

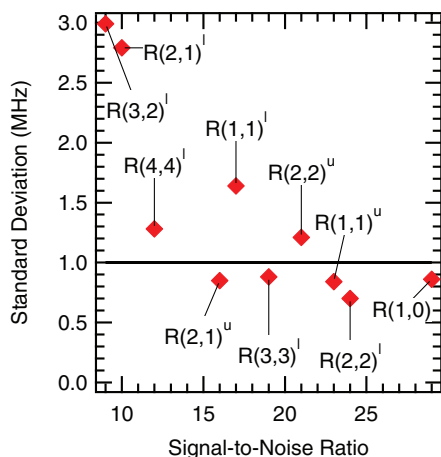| Transition	Error (MHz)
R(1,1)^l	− 5.75
R(1,0)	11.12
R(1,1)^u	19.65
R(2,2)^l	− 5.03
R(2,1)^l	− 12.42
R(2,2)^u	− 10.75
R(2,1)^u	− 9.43
R(3,3)^l	− 3.54
R(3,2)^l	− 41.24

FIG. 4. The standard deviation of the frequency measurements for each H_3^+ transition plotted against the average signal-to-noise ratio of the blended Lamb dip. The horizontal line at 1 MHz is drawn to indicate that the standard deviation is scattered about it for most transitions.
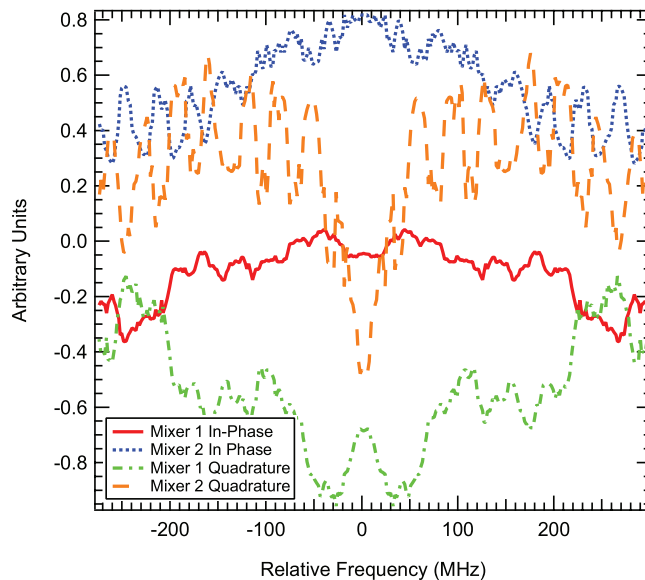

FIG. 5. A typical graph depicting the inversion residuals. It is evident that they are symmetric about the transition frequency, due to the process of additively imprinting the noise of one half of the line on the other. These data are used to calculate characteristic parameters of the asymmetry.

Because of these discrepancies, we have taken great care to characterize potential sources of systematic and random errors in our experiment, as described in Secs. III B 1–III B 4.

1. Effect of signal-to-noise ratio

The precision of the linecenters derived from the fits to our individual scans is typically a few hundred kHz, but can be as low as 70 kHz. Clearly, the fit precision is not the limiting factor in our measurements. To assess the effect of the signal-to-noise ratio of the Lamb dips on our linecenter measurements, the average signal-to-noise ratio of the blended Lamb dips for each transition is plotted against the standard deviation of its linecenter, as determined from several scans over each transition, in Figure 4.

All except the two weakest transitions are clustered near the horizontal line at 1 MHz; these two transitions have fits that are less well determined, which is the cause of the greater uncertainty in their linecenters. No gradual trend in the standard deviation as a function of signal-to-noise ratio is evident, indicating that there is some other dominant effect limiting the standard deviation for all but the weakest lines.

2. Effect of asymmetry

In Crabtree *et al.*,[9] the effect of asymmetry on the determined transition frequency was left as an unanswered question due to the fact that the accuracy was limited to ∼70 MHz by the wavemeter calibration. In that work, several simulated asymmetries were used to intentionally affect the ability to fit the lines, though no physical meaning or mechanism was used in the simulations. The largest magnitude effects were found to cause a few MHz shift in transition frequency, and this was interpreted as a firm upper limit on the potential effect of asymmetry.

With the inclusion of a frequency comb, the effect caused by asymmetry can now be better characterized. For this purpose, the R(1,0) transition was scanned many times on many different days to study the asymmetry. In all cases, the fit

residuals do not indicate any obvious asymmetry in the Lamb dips, which would have the largest effect in the determination of linecenters. Instead, the Doppler profiles clearly exhibit asymmetric lineshapes, and the amount and sign of this asymmetry changes over time and from scan to scan.

To quantify the amount of asymmetry (deviation from the expected odd symmetry) in each scan, we first trimmed each channel of a scan to an equal number of data points on each side of the line center, and shifted it by the y-offset determined from the fit. A copy of the data was made and then the frequency axis was inverted, mirroring the data across the linecenter. The original scan channels and mirrored scan channels were added together to create a graphical representation of the asymmetry (Figure 5), which we refer to as the inversion residuals.

From the inversion residuals, two parameters were determined. The first, the offset asymmetry parameter, was defined as the average value of all four channels. The average value from each individual channel was determined, then these four averages were averaged together. The offset asymmetry parameter was defined in this manner to capture the effect that each individual channel would have on the simultaneous least squares fit of all four channels. In the case of a perfectly symmetric line, the offset parameter would have a value of zero because the odd lineshape would cancel itself out. Negative values of the offset parameter indicate that the lower frequency (negative-going) lobe is stronger than the higher frequency lobe; whereas, positive values indicate stronger lobes on the high frequency side.

The second parameter, which we refer to as the high-low asymmetry parameter, represents the average difference between the maximum and minimum values for each of the four inversion residuals. The high-low parameter is intended to capture an imbalance in the shape of the line. Such an imbalance would manifest itself in the inversion residuals as a
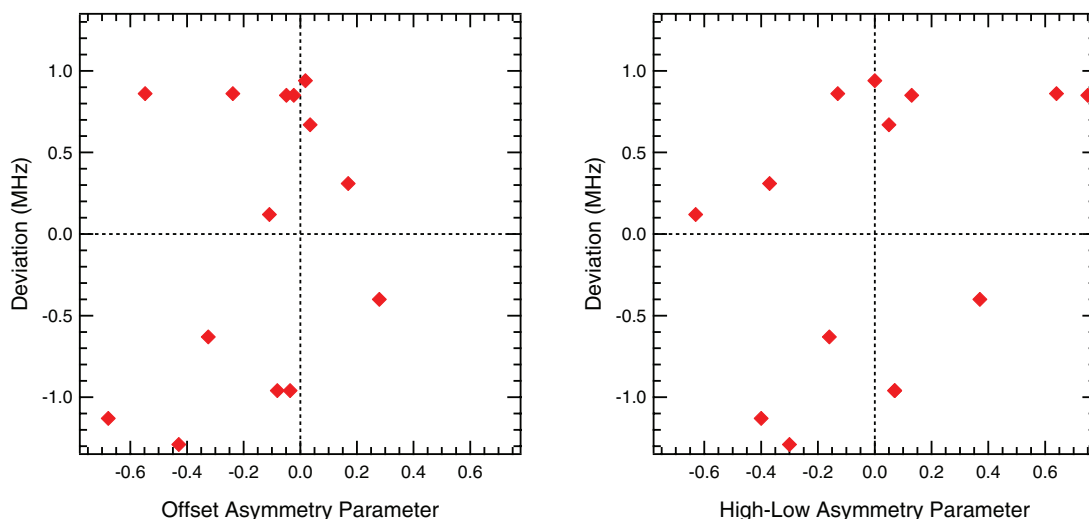
FIG. 6. The deviation of the linecenter of a given scan from the mean value versus the offset asymmetry parameter (left panel) and the high-low asymmetry parameter (right panel). The dotted lines shows the zero crossings to emphasize the insensitivity of the sign of the difference to the sign of the asymmetry parameter.

sloped or curved line. The magnitude of the slope is parameterized by differencing the maximum and minimum values of the residuals. These differences for each data channel are averaged just like the offset parameter. As above, the sign indicates which lobe was larger.

In Figure 6, the deviation of the linecenter of an individual scan from the mean of all R(1,0) scans is plotted against these two asymmetry parameters. The data show no clear trend, not even a consistent change in the sign of the deviation with the sign of the asymmetry parameter. Instead, the data are well scattered. If the scan-to-scan reproducibility in the linecenter of ∼1 MHz is due to the changing asymmetry, it must depend on the asymmetry in a way that is not captured by these particular metrics.

In any case, the fact that the amount and the sign of the asymmetry change from scan to scan strongly suggests that the asymmetry cannot cause a systematic shift in the linecenter in an ensemble of scans. Instead, we conclude that the impact of the asymmetry manifests itself as a random error, reflected in the magnitude of the standard deviation of the linecenter determinations.

3. Pressure shift

Given the difference in pressure between our experiment and Shy's, we decided to measure the linecenter of the R(1,0) transition at three different pressures to rule out the possibility of an unexpectedly large pressure shift. The results are displayed in Table III, and show the same linecenter (within uncertainties) from pressures between 200 and 500 mTorr. The largest pressure shift consistent with the data, determined from the lower bound of the 200 mTorr data (81 720 377.06 MHz) and the upper bound of the 500 mTorr data (81 720 377.86 MHz), would be 2.7 MHz/Torr at the 1σ level. This would mean our linecenter measured at 200 mTorr could be too high by at most 0.4 MHz from the value at 55 mTorr (the midpoint of Shy's range).

4. Comb calibration test

In order to rule out any unexpected problems with the calibration of our optical frequency comb, we wished to measure another transition that had been previously measured with high precision. Since there are no other ion transitions known to this level of accuracy in the mid-infrared, we pursued spectroscopy of neutral methane, which has comb calibrated lines in our spectral region that are known to high accuracy and precision.[24]

Obviously, NICE-OHVMS could not be performed because the instrument cannot modulate the velocity of a neutral molecule. Ordinary NICE-OHMS is challenging to perform with a fiber based EOM due to strong baseline drifts from residual amplitude modulation (RAM),[25, 26] so an additional layer of modulation is necessary. The logical choice was wavelength modulation, but our pump laser must be locked to the comb and our use of an external cavity requires feedback to the OPO cavity length, which fixes the frequency of the signal. Therefore, the cavity was removed and the back reflection detector was used in a double pass configuration for wavelength modulated heterodyne spectroscopy.

Without the need to apply feedback to the OPO cavity length, this control could be used to apply a dither necessary to modulate the wavelength of the signal, and hence also the idler. A 1.4 kHz dither was applied to the cavity, and the lock-in amplifiers were referenced to three times the dither frequency. This allowed the system to be insensitive to the Doppler profile of the methane transition. The chosen target

TABLE III. Measured linecenters of the R(1,0) transition of H_3^+ at different pressures.

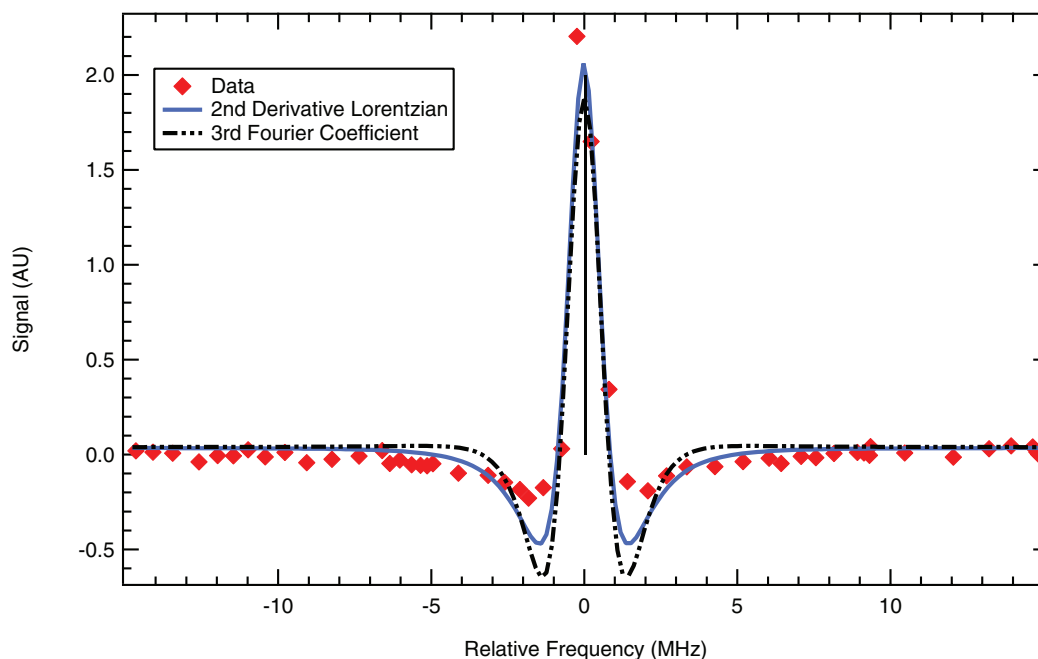| Pressure (mTorr)	Frequency (MHz)
200	81720377.29(23)
350	81720377.47(32)
500	81720377.44(42)

FIG. 7. The comb calibrated central Lamb dip of the $F_1^{(2)}$ component of the P(7) transition in the ν_3 band of methane. Fits to an analytical expression of the third Fourier coefficient for a wavelength modulated dispersion signal (dashed curve) and to the second derivative of a Lorentzian (solid curve) are shown. The black line is the linecenter determined by Takahata *et al.*[24]

was the $F_1^{(2)}$ component of the P(7) transition in the ν_3 band, which has been reported to kHz precision.[24] A few mTorr of methane was leaked into the discharge cell, and the central Lamb dip, which corresponds only to dispersion, was recorded.

The result of our methane spectroscopy is shown in Figure 7. We fit the data to both the third Fourier coefficient for a Lorentzian dispersion lineshape[27] and a simple second derivative of a Lorentzian. While neither fit perfectly reproduces the observed lineshape, the derived linecenters compare very favorably with the previous work of Takahata *et al.*[24] The linecenter as determined by the second derivative fit is 5 ± 22 kHz less than Takahata's, and that from the third Fourier coefficient fit was 10 ± 30 kHz greater than Takahata's. Even by the roughest approximation of simply picking the highest recorded point and calling it the line center, the error is only 222 kHz. Therefore, we conclude that our frequency comb system is working well, and is not the limiting source of error in our ion measurements.

C. HCO⁺ spectroscopy

While there are no molecular ion transitions in the mid-infrared previously measured with sub-MHz accuracy, there are ions (such as HCO⁺) for which pure rotational transitions are known with such accuracy. By measuring multiple rovibrational transitions and using combination differences, we can compare the results with observed rotational transitions as yet another check on the accuracy of our ion transition measurements.

We have recently performed such "indirect rotational spectroscopy" using Doppler-limited spectra of HCO⁺ with comb calibration.[10] Ultimately, we expect this approach to be a useful tool for inferring rotational spectra that have not been directly measured, in order to support astronomical observations with far-infrared/THz instruments such as SOFIA and ALMA. Here, we simply extend our previous work on HCO⁺ to demonstrate the accuracy of our sub-Doppler NICE-OHVMS spectra.

The P(5) and R(3) lines from the ν_1 band of HCO⁺ were measured (see Figure 8) in order to determine the energy level separation between $J = 5$ and $J = 3$ in the ground vibrational state. The two transitions were measured multiple times to determine their linecenters, which were 92 145 080.8(4) MHz for P(5) and 92 947 717.3(5) MHz for R(3). The difference between these frequencies, 802 636.5(7) MHz, agrees within its uncertainty with the sum of the $J = 3 \rightarrow 4$ and $J = 4 \rightarrow 5$ pure rotational transitions observed by Cazzoli *et al.*,[28] 356 734.2230(15) + 445 902.8721(15) = 802 637.0951(21) MHz. The excellent agreement of this combination difference strongly suggests that our experiment does not suffer from any systematic errors that differ from one line to the next, beyond those at the sub-MHz level that result from scan-to-scan variations.

It is interesting to note that the P(5) and R(3) frequencies determined from the Lamb dips are both ∼4 MHz lower than those determined from our earlier Doppler-limited, single-pass measurements.[10] This difference is evidently due to an asymmetry in the drift velocity of the ions on the two half-cycles of the AC discharge; such an asymmetry results in a net Doppler shift in the single-pass measurements, but the present measurements are insensitive to this effect due to the bi-directional nature of the cavity and the fact that the Lamb dips are located symmetrically about the zero-velocity component.
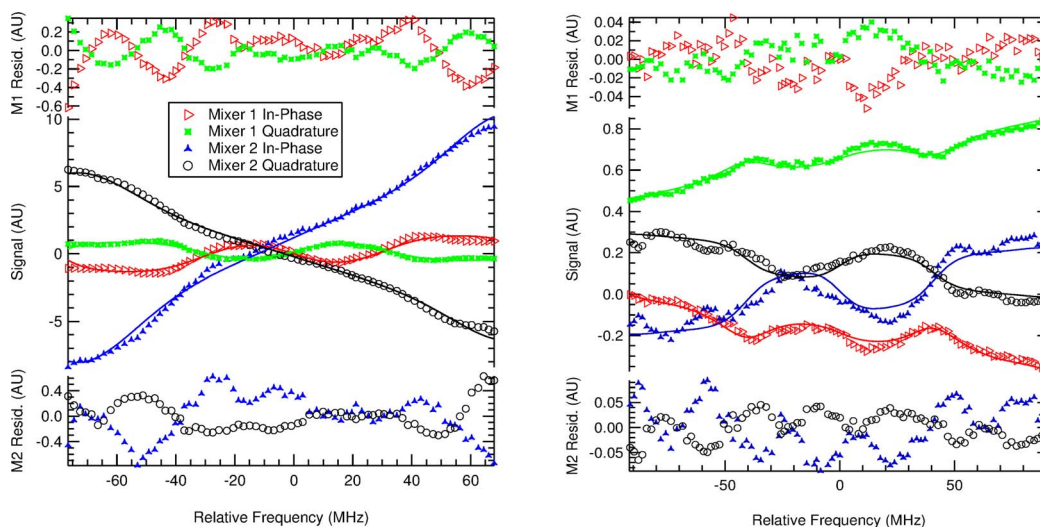
FIG. 8. Results from fitting the Lamb dips from the P(5) transition (left) and R(3) transition (right) of HCO$^+$. The four channels are presented with residuals from each mixer plotted above and below the fit. The data are shown as markers and the fits as solid lines.

D. CH$_5^+$ spectroscopy

An important future application of this technique will be high-precision and high-accuracy spectroscopy of highly congested spectra, such as that of CH$_5^+$. The infrared spectrum of this ion was first reported by the Oka group in 1999,[3] and consisted of about 900 spectral lines between 2770 and 3150 cm^{-1}, with no discernable patterns. The spectrum is complicated by the fact that CH$_5^+$ does not have a single equilibrium structure, but can sample all 5! = 120 equivalent minima of C$_s$ symmetry on its potential energy surface, as well as the C$_s$ and C$_{2v}$ saddle points that interconnect them. Many important theoretical studies (see, e.g., Refs. 29–35) have been undertaken since the publication of Oka's spectrum, and low-resolution spectra have been reported covering different frequency ranges[36] and temperatures.[31] Despite nearly 15 years of effort since the Oka group's first report, the community seems to be no closer to an assignment of Oka's spectrum.

One possible way forward is to search for four-line combination differences in the spectrum, that is, to look for two pairs of transitions with the same combination difference. This would represent an experimental measure of the separation between two rotational energy levels. If spectra with reliable intensities could be obtained at different temperatures, it may be possible to begin assembling an energy level diagram. Comparison between such experimentally determined energy levels and those predicted by sophisticated theoretical techniques might eventually lead to an assignment. However, the frequency uncertainties in the Oka group spectrum range from 90 to 180 MHz, as their measurements were limited by their Doppler linewidth, relatively low signal-to-noise ratio, and traditional frequency calibration techniques (reference gases). Given the line density, there are almost innumerable pairs of transitions whose combination differences agree within this level of uncertainty, and the vast majority of those are accidental rather than true four-line combination differences.

Progress on this front will necessitate remeasurements of CH$_5^+$ transitions with considerably higher accuracy and preci-

sion. The Schlemmer group recently made the first report of a high-resolution spectrum since Oka's, using a cryogenically cooled ion trap and laser-induced reaction spectroscopy.[37] With their smaller Doppler linewidth ($\sim$70 MHz at 20 K) and frequency comb calibration, they determined the central frequency of a CH$_5^+$ transition at 2932.998460 cm^{-1} to within $\sim$200 kHz. An alternative approach, which we are pursuing, is to obtain sub-Doppler spectra in a positive column discharge.

Our experiment uses the same discharge cell that was used for the first report of the CH$_5^+$ spectrum. We are attempting to reproduce the plasma conditions as closely as possible, but the CH$_5^+$ signal is exquisitely sensitive to the exact discharge conditions and we are still in the process of optimizing the system. Nevertheless, we have obtained several comb-calibrated scans of the transition Oka's group reported at 2898.008 cm^{-1}, with a signal-to-noise ratio that is somewhat higher than that of the Oka group. Given our $\sim$10-fold longer effective pathlength (from the cavity enhancement) and the fact that our noise level should be lower than Oka's (because of the frequency modulation), we suspect that further tuning of plasma conditions should lead to significantly stronger signals.

The average of five spectra of this transition is displayed in Figure 9, and represents the first sub-Doppler spectrum of CH$_5^+$. A fit to the averaged spectrum yields a linecenter of 86 880 178.469(126) MHz; the precision of this fit is more than two orders of magnitude lower than the $\sim$90 MHz uncertainty from the Oka group's measurements. The Schlemmer group has independently measured a CH$_5^+$ line centered at 86 880 178.22(63) MHz.[38] This transition is only $\sim$240 kHz different from our measurement, which agrees with our transition frequency within 1σ of their uncertainty and 2σ of our uncertainty. This provides independent confirmation of the accuracy of our technique. The weakness of the CH$_5^+$ Lamb dip, compared to those seen in H$_3^+$ and HCO$^+$, is likely the result of the lower transition dipole moment of CH$_5^+$. Although we are not aware of any predictions for the transition dipole moment, the MULTIMODE calculations of Huang *et al.*[31] show
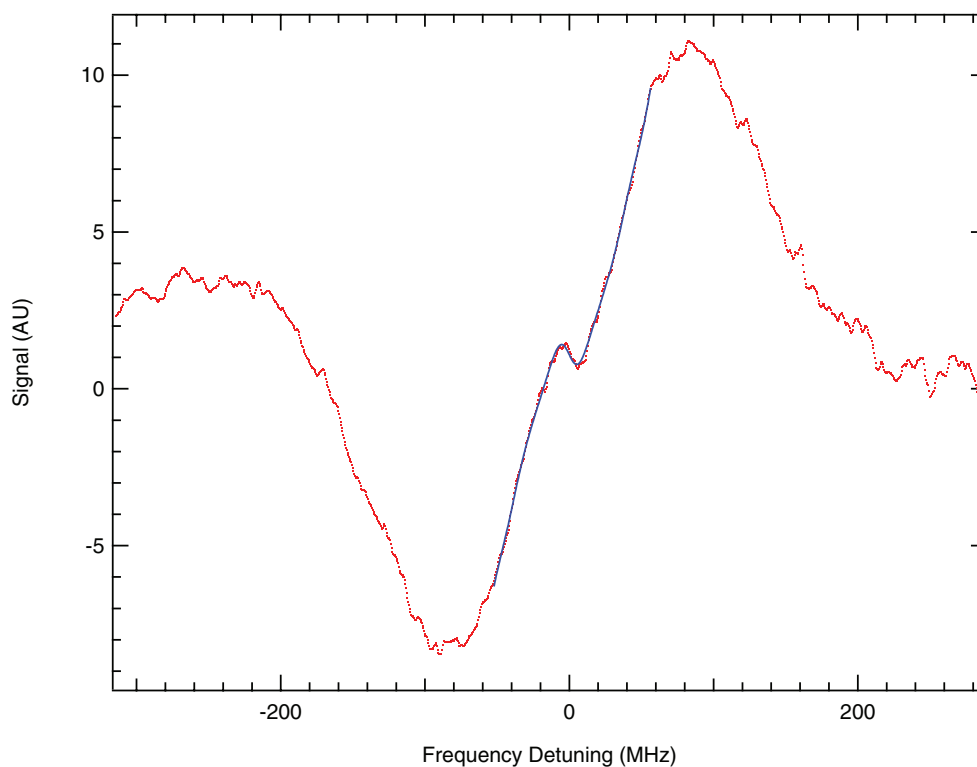
FIG. 9. Comb-calibrated NICE-OHVMS spectrum of Oka's "2898.008 cm^{-1}" transition of CH$_5^+$. The data are shown as red dots and the fit to the Lamb dip is shown as a blue line.

an integrated band intensity of $\sim$50 km/mol, which is considerably lower than the calculated value of 227 km/mol[39] for HCO$^+$.

In the future, we hope to increase the Lamb dip depth by increasing the power injected into our cavity and/or by obtaining mirrors with higher reflectivity. Even if this is not effective, we expect to be able to improve the signal-to-noise ratio on the Lamb dip by further optimization of the plasma conditions and by reducing technical noise sources in our spectrometer.

IV. CONCLUSIONS

We have demonstrated the first instrument capable of routine sub-Doppler spectroscopy of a wide variety of molecular ions, offering both high precision from optical saturation and high accuracy from optical frequency comb calibration. Using this instrument, ten lines of the doubly degenerate ν_2 band of H$_3^+$ have been measured, eight of which have sub-MHz uncertainties. Two lines from the ν_1 band of HCO$^+$ have also been measured with similar uncertainties, and their combination difference is in excellent agreement with pure rotational spectroscopy. The first sub-Doppler spectrum of CH$_5^+$ has also been recorded with sub-MHz precision, a substantial improvement over the $\sim$90 MHz uncertainty of the initial detection in the Oka group.[3]

Because our measurements of H$_3^+$ transitions disagree with those reported by Shy's group[22,23] by $\sim$5 MHz, we have conducted an extensive analysis of potential sources of experimental error in our instrument. The limiting factor in our

frequency determinations appears to be scan-to-scan variability that is not yet understood, but results in a standard deviation among individual scans of $\sim$1 MHz. The standard error of a set of scans can be reduced to $\sim$250 kHz by performing multiple scans. The scan-to-scan variability may be due to varying asymmetry of the Doppler-broadened lineshape, but our attempts to find correlations between the center frequency deviations and measures of the asymmetry have not been successful. All indications are that our determined standard errors accurately capture the random errors in our measurements. This conclusion is further supported by the excellent combination difference between the HCO$^+$ transitions we measured. We have also excluded the possibility of systematic errors due to pressure shift, and we have confirmed the accuracy of our frequency comb calibration within tens of kHz using a known transition of methane. Most importantly, the independent measurement of the same CH$_5^+$ transition by Schlemmer's group[38] is the strongest evidence that our technique does not exhibit errors of order 5 MHz, which provides us with the utmost confidence in the values that we have reported.

The instrument is currently limited in wavelength coverage by the coverage of our OPO module (3.2–3.9 μm), and to some extent by the coatings of our external cavity mirrors (nominally 3.0–3.4 μm, but usable outside this range). However, OPO modules are available that cover 2.3–4.6 μm, and it should be possible to produce moderate reflectivity ($\sim$99.0–99.7%) cavity mirrors across that range. Considering the chemical versatility of the positive column discharge and the general applicability of direct absorption/dispersion spectroscopy, our technique will enable the high-precision,

high-accuracy spectroscopy of a wide variety of molecular ions. Possible applications include tests of high accuracy *ab initio* calculations, supporting astronomical observations, and aiding in the assignment of congested spectra.

[1]C. Gudeman, M. Begemann, J. Pfaff, and R. Saykally, Phys. Rev. Lett. **50**, 727 (1983).

[2]S. K. Stephenson and R. J. Saykally, Chem. Rev. **105**, 3220 (2005).

[3]E. T. White, J. Tang, and T. Oka, Science **284**, 135 (1999).

[4]T. Amano, J. Chem. Phys. **79**, 3595 (1983).

[5]A. A. Mills, B. M. Siller, and B. J. McCall, Chem. Phys. Lett. **501**, 1 (2010).

[6]B. M. Siller, A. A. Mills, and B. J. McCall, Opt. Lett. **35**, 1266 (2010).

[7]B. M. Siller, M. W. Porambo, A. A. Mills, and B. J. McCall, Opt. Express **19**, 24822 (2011).

[8]L.-S. Ma, J. Ye, P. Dubé, and J. L. Hall, J. Opt. Soc. Am. B **16**, 2255 (1999).

[9]K. N. Crabtree, J. N. Hodges, B. M. Siller, A. J. Perry, J. E. Kelly, P. A. Jenkins, and B. J. McCall, Chem. Phys. Lett. **551**, 1 (2012).

[10]B. M. Siller, J. N. Hodges, A. J. Perry, and B. J. McCall, "Indirect rotational spectroscopy of HCO^+," J. Phys. Chem. A **117**(39), 10034–10040 (2013).

[11]M. Pavanello, L. Adamowicz, A. Alijah, N. F. Zobov, I. I. Mizus, O. L. Polyansky, J. Tennyson, T. Szidarovszky, A. G. Császár, M. Berg, A. Petrignani, and A. Wolf, Phys. Rev. Lett. **108**, 023002 (2012).

[12]J. Komasa, K. Piszczatowski, G. Łach, M. Przybytek, B. Jeziorski, and K. Pachucki, J. Chem. Theory Comput. **7**, 3105 (2011).

[13]P. Pyykkö, K. Dyall, A. Császár, G. Tarczay, O. Polyansky, and J. Tennyson, Phys. Rev. A **63**, 024502 (2001).

[14]T. R. Geballe and T. Oka, Nature **384**, 334 (1996).

[15]N. Indriolo and B. J. McCall, Astrophys. J. **745**, 91 (2012).

[16]P. Drossart, J.-P. Maillard, J. Caldwell, S. J. Kim, J. K. G. Watson, W. A. Majewski, J. Tennyson, S. Miller, S. K. Atreya, J. T. Clarke, J. H. Waite, and R. Wagener, Nature **340**, 539 (1989).

[17]D. Rego, N. Achilleos, T. Stallard, and S. Miller, Nature **399**, 121 (1999).

[18]C. Savage, F. Dong, and D. J. Nesbitt, in *60th International Symposium on Molecular Spectroscopy, Talk MG06* (2005).

[19]K.-Y. Wu, "Precision Measurement of the ν_2-band of triatomic hydrogen molecular ion H_3^+," Ph.D. thesis, National Tsing Hua University, 2008.

[20]A. McKellar and J. Watson, J. Mol. Spectrosc. **191**, 215 (1998).

[21]T. Oka, Philos. Trans. R. Soc. London, Ser. A **303**, 543 (1981).

[22]H.-C. Chen, C.-Y. Hsiao, J.-L. Peng, T. Amano, and J.-T. Shy, Phys. Rev. Lett. **109**, 263002 (2012).

[23]H.-C. Chen, J.-L. Peng, T. Amano, and J.-T. Shy, in *68th International Symposium on Molecular Spectroscopy, Talk MG05* (2013).

[24]K. Takahata, T. Kobayashi, H. Sasada, Y. Nakajima, H. Inaba, and F.-L. Hong, Phys. Rev. A **80**, 032518 (2009).

[25]A. Foltynowicz, W. Ma, and O. Axner, Opt. Express **16**, 14689 (2008).

[26]A. Foltynowicz, I. Silander, and O. Axner, J. Opt. Soc. Am. B **28**, 2797 (2011).

[27]J. Westberg, P. Kluczynski, S. Lundqvist, and O. Axner, J. Quant. Spectrosc. Radiat. Transf. **112**, 1443 (2011).

[28]G. Cazzoli, L. Cludi, G. Buffa, and C. Puzzarini, Astrophys. J., Suppl. Ser. **203**, 11 (2012).

[29]P. R. Bunker, B. Ostojić, and S. Yurchenko, J. Mol. Struct. **695–696**, 253 (2004).

[30]Z. Jin, B. J. Braams, and J. M. Bowman, J. Phys. Chem. A. **110**, 1569 (2006).

[31]X. Huang, A. B. McCoy, J. M. Bowman, L. M. Johnson, C. Savage, F. Dong, and D. J. Nesbitt, Science **311**, 60 (2006).

[32]M. P. Deskevich, A. B. McCoy, J. M. Hutson, and D. J. Nesbitt, J. Chem. Phys. **128**, 094306 (2008).

[33]C. E. Hinkle and A. B. McCoy, J. Phys. Chem. A **112**, 2058 (2008).

[34]X.-G. Wang and T. Carrington, Jr., J. Chem. Phys. **129**, 234102 (2008).

[35]C. E. Hinkle, A. S. Petit, and A. B. McCoy, J. Mol. Spectrosc. **268**, 189 (2011).

[36]O. Asvany, P. Kumar, B. Redlich, I. Hegemann, S. Schlemmer, and D. Marx, Science **309**, 1219 (2005).

[37]O. Asvany, J. Krieg, and S. Schlemmer, Rev. Sci. Instrum. **83**, 093110 (2012).

[38]S. Schlemmer, private communication (2013).

[39]J. M. L. Martin, P. R. Taylor, and T. J. Lee, J. Chem. Phys. **99**, 286 (1993).